

# Phase transition in a two-dimensional triangular flow with consideration of optimal current difference effect

Poonam Redhu · Arvind Kumar Gupta

Received: 19 March 2014 / Accepted: 23 May 2014 / Published online: 17 June 2014  
© Springer Science+Business Media Dordrecht 2014

**Abstract** A modified two-dimensional triangular lattice model is presented by accounting the effect of optimal current difference on traffic dynamics and analyzed both theoretically and numerically. Based on the sensitivity and configurations of vehicles, two distinct types of jamming transitions occur: conventional jamming transition to the kink jam and jamming transition to the chaotic jam through kink jam. The chaotic region reduces with reaction coefficient and enhances when more number of vehicles move diagonally. It is shown that the incorporation of optimal current difference effect efficiently stabilizes the traffic flow and suppresses traffic jam for all possible configurations on triangular lattice.

**Keywords** Traffic flow · Optimal current difference · Triangular lattice · Chaotic flow

## 1 Introduction

With the rapid development of urbanization, the problem of traffic congestion has been attracted considerable attention of scientists and researchers nowadays. A

variety of models have been applied to describe the collective properties of traffic flow [1–9]. In the last few years, the lattice hydrodynamic traffic model, firstly, proposed by Nagatani [10] has been given much attention. Afterward, many extensions have been carried out by considering different factors like backward effect [11], lateral effect of the lane width [12], density difference effect [13], anticipation effect of potential lane changing [14], optimal current difference effect [15], etc. All of the above-mentioned models describe some traffic phenomena only on a single-lane or two-lane highway.

Most of the road networks, for example, either traffic system of a whole a city or an expressway network, comprise of two or more lanes. So, one-dimensional traffic flow models are not appropriate to study the traffic flow on networks. Therefore, higher dimensional lattice hydrodynamic models, which are very abstract models of traffic flow, can describe the traffic behavior on networks. In this direction, firstly, Biham et al. [16] proposed a two-dimensional traffic flow model by using cellular automata approach. Later, Nagatani extended his one-dimensional lattice hydrodynamic model to two-dimensional [17] as well as to higher dimensional [18] traffic flow models. Recently, Gupta and Redhu [19] investigated the effect of optimal current difference in a two-dimensional traffic flow model on square lattice.

In order to make two-dimensional square lattice model more appropriate in explaining traffic dynamics on networks, Nagatani [20], further, studied two-

---

P. Redhu · A. K. Gupta (✉)  
Indian Institute of Technology Ropar,  
Rupnagar 140001, Punjab, India  
e-mail: ak Gupta@iitrpr.ac.in

P. Redhu  
e-mail: poonamr@iitrpr.ac.in

dimensional triangular lattice model by assuming three types of vehicles and observed that jamming transition in traffic flow depends on the lattice type. However, best to our knowledge, the effect of optimal current difference on two-dimensional triangular lattice has not been investigated yet.

In this letter, a new two-dimensional triangular lattice model is proposed by considering the effect of optimal current difference. Linear and nonlinear stability analysis will be carried out to investigate the impact of optimal current difference on triangular lattice. Here, we would like to discuss three main points: (1) To check whether or not the modified model exhibits the similar jamming transition as observed by Nagatani [20]. (2) The effect of optimal current difference on the stability of two-dimensional triangular traffic flow has to be analyzed. (3) To compare the results of triangular and square lattice in two-dimensional traffic flow. Finally, to validate the theoretical findings, numerical simulation will be carried out.

## 2 Proposed model

The lattice hydrodynamic model proposed by Nagatani [10] is the simplified version of continuum traffic flow models incorporating both the ideas of car following and macroscopic models to analyze the density waves. Later, the lattice model was extended to analyze two-dimensional traffic flow on square and triangular lattices by Nagatani [17,20].

However, the above models are able to explain the phase transition and critical phenomena on one- or higher dimensional traffic flow, the important aspect of optimal current difference effect, recently observed by Gupta and Redhu [19], has not been explored yet. To investigate the effect of optimal current difference, we propose a modified model by considering three types of vehicles, where first, second, and third type of vehicles move in the positive  $x$ ,  $y$ , and along diagonal direction, respectively. The interface among three types of vehicles occurs only on the crossing, and vehicles are not allowed to turn. The number of vehicles of each type remains conserved, i.e., one type of vehicles never changes to another type of vehicles. The density [speed] of vehicles moving in the  $x$ ,  $y$ , and along diagonal direction are denoted by  $\rho_x(x, y, t)[u(x, y, t)]$ ,  $\rho_y(x, y, t)[v(x, y, t)]$ , and  $\rho_r(x, y, t)[w(x, y, t)]$ , respectively. Hence, the conti-

nuity equations on two-dimensional triangular lattice are given by

$$\partial_t \rho_x(x, y, t) + \partial_x(\rho_x(x, y, t)u(x, y, t)) = 0, \quad (1)$$

$$\partial_t \rho_y(x, y, t) + \partial_y(\rho_y(x, y, t)v(x, y, t)) = 0, \quad (2)$$

$$\partial_t \rho_r(x, y, t) + \partial_r(\rho_r(x, y, t)w(x, y, t)) = 0, \quad (3)$$

where  $\partial_t = \partial/\partial t$ ,  $\partial_x = \partial/\partial x$ ,  $\partial_y = \partial/\partial y$ , and  $\partial_r = \partial/\partial r$ .

In real traffic, drivers always adjust their velocity according to the observed traffic situations and estimate their driving behavior. We propose new evolution equations for two-dimensional triangular lattice with the consideration of optimal current difference as follows:

$$\begin{aligned} \rho_x(x, y, t + \tau)u(x, y, t + \tau) \\ = c_x \rho_0[V(\rho(x + h, y, t))] + \lambda c_x \rho_0[V(\rho(x + 2h, y, t)) \\ - V(\rho(x + h, y, t))], \end{aligned} \quad (4)$$

$$\begin{aligned} \rho_y(x, y, t + \tau)v(x, y, t + \tau) = c_y \rho_0[V(\rho(x, y + h, t))] \\ + \lambda c_y \rho_0[V(\rho(x, y + 2h, t)) \\ - V(\rho(x, y + h, t))], \end{aligned} \quad (5)$$

$$\begin{aligned} \rho_r(x, y, t + \tau)w(x, y, t + \tau) = c_r \rho_0[V(\rho(x + h, y + h, t))] \\ + \lambda c_r \rho_0[V(\rho(x + 2h, y + 2h, t)) \\ - V(\rho(x + h, y + h, t))], \end{aligned} \quad (6)$$

where  $\rho(x, y, t) = \rho_x(x, y, t) + \rho_y(x, y, t) + \rho_r(x, y, t)$ ;  $\rho_0$  is the total average density;  $h$  is the average headway;  $c_x$ ,  $c_y$ , and  $c_r$  are the fractions of vehicles moving in  $x$ ,  $y$ , and along diagonal direction, respectively;  $\lambda$  is the reaction coefficient of optimal current difference;  $V(\cdot)$  is the optimal velocity function; and  $\tau$  ( $a = 1/\tau$ ) is the delay that requires to reach the traffic current at optimal level. In the proposed model, the traffic current in the  $x$ -direction at position  $(x, y)$  at time  $t$  is adjusted not only by the optimal current at position  $(x + h, y)$  at time  $t - \tau$ , but also affected by the optimal current difference at  $(x + 2h, y)$  and  $(x + h, y)$  at time  $t - \tau$ . Combining the difference form of Eqs.(1), (2), and (3) with Eqs. (4), (5), and (6), the modified lattice hydrodynamic model is obtained as follows:

$$\begin{aligned} \rho_{j,m}(t + 2\tau) - \rho_{j,m}(t + \tau) + \tau \rho_0^2 c_x [V(\rho_{j+1,m}) \\ - V(\rho_{j,m})] + \tau \rho_0^2 c_y [V(\rho_{j,m+1}) - V(\rho_{j,m})] \\ + \tau \rho_0^2 c_r [V(\rho_{j+1,m+1}) - V(\rho_{j,m})] \\ + \lambda \tau \rho_0^2 c_x [V(\rho_{j+2,m}) - 2V(\rho_{j+1,m}) + V(\rho_{j,m})] \end{aligned}$$

$$\begin{aligned}
 & + \lambda \tau \rho_0^2 c_y [V(\rho_{j,m+2}) - 2V(\rho_{j,m+1}) + V(\rho_{j,m})] \\
 & + \lambda \tau \rho_0^2 c_r [V(\rho_{j+2,m+2}) \\
 & - 2V(\rho_{j+1,m+1}) + V(\rho_{j,m})] = 0, \tag{7}
 \end{aligned}$$

where  $\rho_{j,m}(t) = \rho_{x,j,m}(t) + \rho_{y,j,m}(t) + \rho_{r,j,m}(t)$ ;  $\rho_{x,j,m}(t)$ ,  $\rho_{y,j,m}(t)$ , and  $\rho_{r,j,m}(t)$  are the densities, respectively, in  $x$ ,  $y$ , and along diagonal directions at the site  $(j, m)$  on the triangular lattice. For  $c_r = 0$ , the above modified model reduces to two-dimensional model on a square lattice, recently proposed by Gupta and Redhu [19], in which the reaction coefficient of optimal current difference effectively suppresses the traffic jam for all the possible configurations of vehicles. Furthermore, when  $\lambda = 0$ , the model reduces to two-dimensional triangular lattice as presented by Nagatani [20]. The optimal velocity function is adopted as following [20]:

$$V(\rho_{j,m}) = 1 - \tanh\left(\frac{\rho_{j,m}(t) - \rho_c}{\rho_0^2}\right), \tag{8}$$

where  $\rho_c$  denotes the safety critical density. The optimal velocity function, which is monotonically decreasing, has an upper bound (maximal velocity) and a turning point at  $\rho_{j,m} = \rho_c = \rho_0$ .

### 3 Linear stability analysis

We perform the linear analysis to study the stability of two-dimensional model on a triangular lattice. For this, the state of uniform traffic flow is taken as  $\rho_0$  and optimal velocity  $V(\rho_0)$ , where  $\rho_0$  is a constant. Hence, the steady-state solution of the homogeneous traffic flow is given by

$$\rho_{j,m}(t) = \rho_0, \text{ and } V_{j,m}(t) = V(\rho_0).$$

Let  $y_{j,m}(t)$  be a small deviation from the steady-state flow  $\rho_{j,m}(t) = \rho_0 + y_{j,m}(t)$ .

Substituting perturbed density profile into Eq. (7) and linearizing it, we obtain

$$\begin{aligned}
 & y_{j,m}(t + 2\tau) - y_{j,m}(t + \tau) \\
 & + \tau \rho_0^2 V'(\rho_0) c_x [y_{j+1,m}(t) - y_{j,m}(t)] \\
 & + \tau \rho_0^2 V'(\rho_0) c_y [y_{j,m+1}(t) - y_{j,m}(t)] \\
 & + \tau \rho_0^2 V'(\rho_0) c_r [y_{j+1,m+1}(t) - y_{j,m}(t)] \\
 & + \lambda \tau \rho_0^2 V'(\rho_0) c_x [y_{j+2,m}(t) - 2y_{j+1,m}(t) + y_{j,m}]
 \end{aligned}$$

$$\begin{aligned}
 & + \lambda \tau \rho_0^2 V'(\rho_0) c_y [y_{j,m+2}(t) - 2y_{j,m+1}(t) + y_{j,m}] \\
 & + \lambda \tau \rho_0^2 V'(\rho_0) c_r [y_{j+2,m+2}(t) \\
 & - 2y_{j+1,m+1}(t) + y_{j,m}] = 0, \tag{9}
 \end{aligned}$$

where  $V'(\rho_0) = \frac{dV(\rho)}{d\rho}|_{\rho=\rho_0}$ . Putting  $y_{j,m}(t) = e^{ik(j+m)+zt}$  in Eq. (9), we obtain

$$\begin{aligned}
 & e^{2\tau z} - e^{\tau z} + \tau \rho_0^2 V'(c_x + c_y)[e^{ik} - 1] \\
 & + \tau \rho_0^2 V' c_r [e^{2ik} - 1] + \lambda \tau \rho_0^2 V'(c_x + c_y)[e^{ik} - 1]^2 \\
 & + \lambda \tau \rho_0^2 V' c_r [e^{2ik} - 1]^2 = 0. \tag{10}
 \end{aligned}$$

Inserting  $z = z_1(ik) + z_2(ik)^2 \dots$  into Eq. (10), we obtained the first and second-order terms of the coefficient  $ik$  and  $(ik)^2$ , respectively, as follows:

$$z_1 = -\rho_0^2 V'(\rho_0)(c_x + c_y + 2c_r), \tag{11}$$

$$\begin{aligned}
 z_2 = & -\frac{3\tau z_1^2}{2} - \frac{\rho_0^2 V'(\rho_0)}{2}(c_x + c_y + 4c_r) \\
 & - \lambda \rho_0^2 V'(\rho_0)(c_x + c_y + 4c_r). \tag{12}
 \end{aligned}$$

When  $z_2 < 0$ , the uniform steady-state flow becomes unstable for long-wavelength waves. For  $z_2 > 0$ , the uniform flow will remain stable.

Thus, the neutral stability curve is given by

$$\tau = -\frac{(1 + 2\lambda)(c_x + c_y + 4c_r)}{3\rho_0^2 V'(\rho_0)(c_x + c_y + 2c_r)^2}. \tag{13}$$

The instability condition for the homogeneous traffic flow can be described as follows:

$$\tau > -\frac{(1 + 2\lambda)(c_x + c_y + 4c_r)}{3\rho_0^2 V'(\rho_0)(c_x + c_y + 2c_r)^2}. \tag{14}$$

It is clear from the Eq. (14) that the stability of traffic flow on a triangular lattice depends on the reaction coefficient as well as on configurations of vehicles on triangular lattice. When  $\lambda = 0$ , i.e., if there is no optimal current difference effect, the stability criteria are same as that of Ref. [20]. Figure 1 represents the phase space plot corresponding to three different configurations of vehicles, where solid (dotted) curves are the neutral (coexisting) stability curves through linear (nonlinear) analysis in the phase space  $(\rho, a)$  for different values of  $\lambda$ . The apex of each curve indicates the critical point  $(\rho_c, a_c)$ . The phase plane is divided into three regions: stable, metastable, and unstable. It can be easily

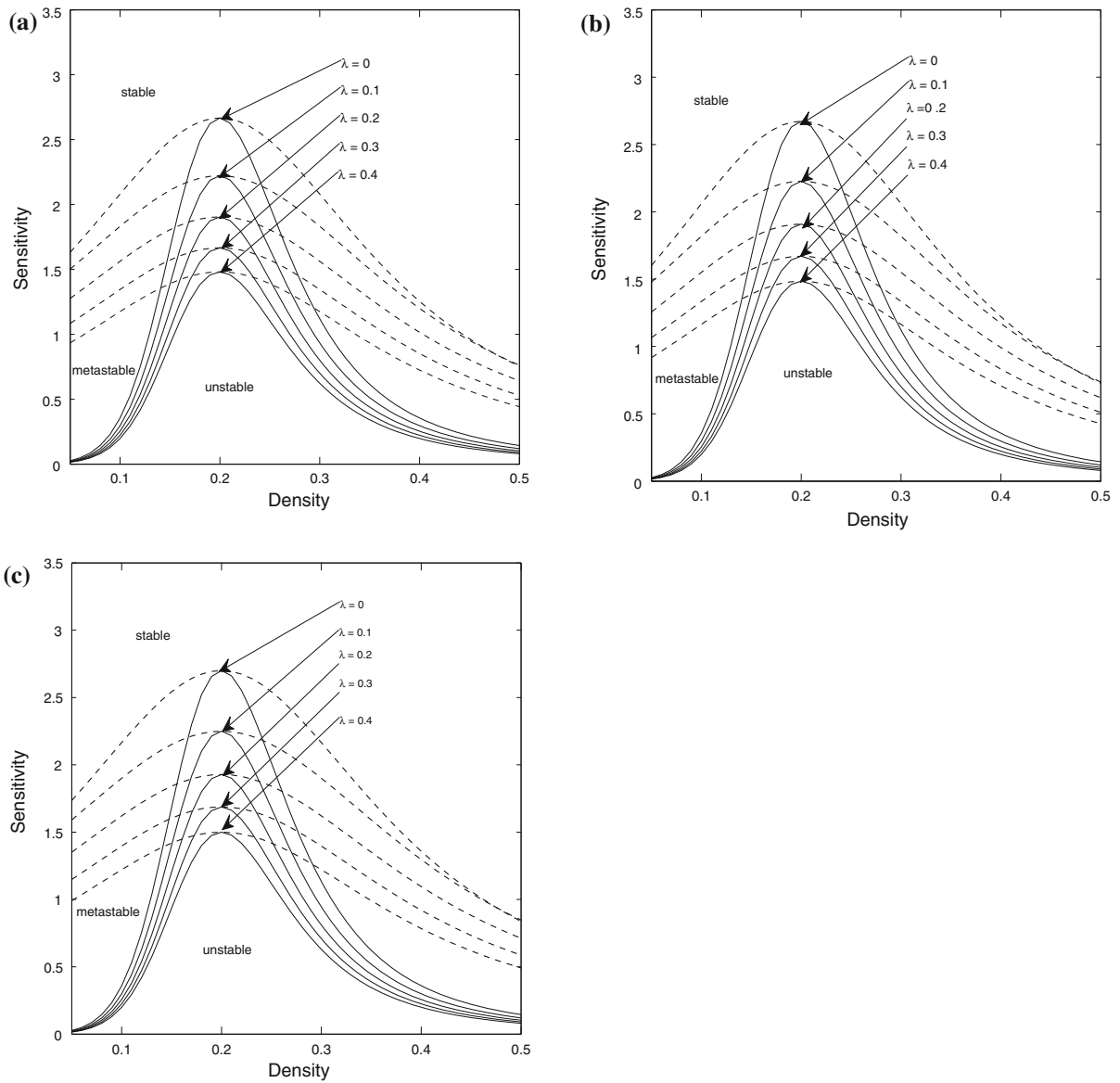


**Fig. 1** Phase diagram in parameter space  $(\rho, a)$  for **a**  $c_x = c_y = c_r = \frac{1}{3}$ , **b**  $c_x = 0.2, c_y = c_r = 0.4$  and **c**  $c_x = c_y = 0.4, c_r = 0.2$ , respectively

observed from the Fig. 1 the amplitude of each curve, i.e., the sensitivity of critical point decreases with an increase in reaction coefficient which means that larger value of  $\lambda$  leads to the enlargement of stable region for all three different configurations on a triangular lattice.

Furthermore, on comparing Fig. 1a, b and c, it can be concluded that the increase in the number of vehicles along the diagonal leads to the enlargement of unstable region. Therefore, it is worth to mention that the stability of traffic flow on a triangular lattice depends

significantly on the reaction coefficient as well as on the configurations of vehicles moving direction.

#### 4 Nonlinear analysis

In this section, we investigate the evolution characteristics by using the method of long-wavelength expansion to describe the collective motion on coarse-grained scales. Assuming,  $X = \epsilon(j + m + bt)$  and  $T = \epsilon^3 t$  as

the slow variables for scaling parameter  $\epsilon$  ( $0 < \epsilon \ll 1$ ) near the critical point, where  $b$  is a constant to be determined, let the density at  $(j, m)$  site near the critical point be

$$\rho_{j,m}(t) = \rho_c + \epsilon R(X, T) \tag{15}$$

By expanding Eq. (7) to fifth order of  $\epsilon$  with the help of Eq. (15), we obtain the following nonlinear equation:

$$\begin{aligned} &\epsilon^2 [b + \rho_c^2 V'(c_x + c_y + 2c_r)] \partial_X R \\ &+ \epsilon^3 \left[ \frac{3b^2 \tau}{2} + \frac{\rho_c^2 V'(c_x + c_y + 4c_r)(1 + 2\lambda)}{2} \right] \partial_X^2 R \\ &+ \epsilon^4 \left[ \partial_T R + \left( \frac{7b^3 \tau^2}{6} + \frac{\rho_c^2 V'(c_x + c_y + 8c_r)(1 + 6\lambda)}{6} \right) \partial_X^3 R \right. \\ &\quad \left. + \frac{\rho_c^2 V'''(c_x + c_y + 2c_r)}{6} \partial_X R^3 \right] \\ &+ \epsilon^5 \left[ 3b\tau \partial_T \partial_X R + \left( \frac{5b^4 \tau^3}{8} + \frac{\rho_c^2 V'(c_x + c_y + 16c_r)(1 + 14\lambda)}{24} \right) \partial_X^4 R \right. \\ &\quad \left. + \frac{\rho_c^2 V'''(c_x + c_y + 4c_r)(1 + 2\lambda)}{12} \partial_X^2 R^3 \right] = 0, \end{aligned} \tag{16}$$

where  $V' = \frac{dV(\rho)}{d\rho}|_{\rho=\rho_c}$  and  $V''' = \frac{d^3V(\rho)}{d\rho^3}|_{\rho=\rho_c}$ . In the neighborhood of critical point  $\tau_c$ , we define

$$\tau = \tau_c(1 + \epsilon^2), \tag{17}$$

and choose  $b = -\rho_c^2 V'(c_x + c_y + 2c_r)$ . Eliminating second and third order terms of  $\epsilon$  into Eq. (16), we get

$$\begin{aligned} &\epsilon^4 (\partial_T R - g_1 \partial_X^3 R + g_2 \partial_X R^3) \\ &+ \epsilon^5 (g_3 \partial_X^2 R + g_4 \partial_X^4 R + g_5 \partial_X^2 R^3) = 0, \end{aligned} \tag{18}$$

where the coefficients  $g_i$  ( $i = 1, 2, \dots, 5$ ) are shown in Table 1. In order to derive the standard mKdV equation, we make the following transformations in

Eq. (16):

$$T' = g_1 T, \quad R = \sqrt{\frac{g_1}{g_2}} R', \tag{19}$$

which gives

$$\partial_T R' - \partial_X^3 R' + \partial_X R'^3 + \epsilon M[R'] = 0, \tag{20}$$

where  $M[R'] = \frac{1}{g_1} \left( g_3 \partial_X^2 R' + \frac{g_1 g_5}{g_2} \partial_X^2 R'^3 + g_4 \partial_X^4 R' \right)$ . After ignoring the  $O(\epsilon)$  terms in Eq. (20), we get the standard mKdV equation whose desired kink soliton solution is given by

$$R'_0(X, T') = \sqrt{c} \tanh \sqrt{\frac{c}{2}} (X - cT'). \tag{21}$$

In order to determine the value of propagation velocity for the kink–antikink solution, it is necessary to satisfy the solvability condition:

$$(R'_0, M[R'_0]) \equiv \int_{-\infty}^{\infty} dX R'_0 M[R'_0] = 0, \tag{22}$$

with  $M[R'_0] = M[R']$ . By solving Eq. (22), the selected value of  $c$  is

$$c = \frac{5g_2 g_3}{2g_2 g_4 - 3g_1 g_5}. \tag{23}$$

Hence, the kink–antikink solution is given by

$$\rho_{j,m}(t) = \rho_c + \epsilon \sqrt{\frac{g_1 c}{g_2}} \tanh \left( \sqrt{\frac{c}{2}} (X - c g_1 T) \right), \tag{24}$$

**Table 1** The coefficients  $g_i$  of the model

$g_1$	$g_2$	$g_3$
$\left( -\frac{7(1+2\lambda)^2(c_x+c_y+4c_r)^2}{54(c_x+c_y+2c_r)} + \frac{(1+6\lambda)(c_x+c_y+8c_r)}{6} \right) (-\rho_c^2 V')$		
$g_4$	$g_5$	
$\left( \frac{5(1+2\lambda)^3(c_x+c_y+4c_r)^3}{216(c_x+c_y+2c_r)^2} + \frac{(c_x+c_y+16c_r)(1+14\lambda)}{24} \right) \rho_c^2 V'$		$\left( \frac{(c_x+c_y+4c_r)(1+2\lambda)}{12} - \frac{(1+2\lambda)(c_x+c_y+4c_r)}{6} \right) \rho_c^2 V'''$

with  $\epsilon^2 = \frac{ac}{a} - 1$  and the amplitude  $A$  of the solution is

$$A = \sqrt{\frac{g_1}{g_2} \epsilon^2 c}. \tag{25}$$

The kink–antikink solution represents the coexisting phase including both freely moving phase and congested phase which can be described by  $\rho_j = \rho_c \pm A$ , respectively, in the phase space  $(\rho, a)$ .

### 5 Numerical simulation

To check the applicability of the modified model and validate the theoretical results in describing traffic flow dynamics on a triangular lattice, numerical simulation is carried out under periodic boundary conditions. Initially, the vehicle density is assumed to be disturbed uniformly over the triangular lattice as  $\rho_{j,m}(0) = \rho_{j,m}(1) = \rho_0$ . Then, the local densities at site  $(L/2, L/2)$  and  $((L/2) - 1, (L/2) - 1)$  for first two time steps are set as  $\rho_0 - \sigma$  and  $\rho_0 + \sigma$ , respectively. Here,  $\rho_0 = 0.2$ ,  $L$  is the system size taken as  $100 \times 100$  and  $\sigma = 0.1$  is the initial disturbance. As observed in the previous section, the behavior of traffic flow significantly depends on the two important parameters: configuration of vehicles and reaction coefficient, and we discuss our findings for three different configurations.

#### Case 1 $c_x = c_y = c_r$

In this case, equal number of vehicles is allowed to move in three possible directions. Figure 2 shows the traffic pattern for different values of  $\lambda$  after a sufficiently long time, namely,  $6 \times 10^4 s$  for  $a = 1.5$ . The initial disturbance added at the center of lattice leads to the kink soliton density waves as shown in Fig. 2a–d, and these density waves propagate in the backward direction with a constant speed in evolution of time. This small amplitude disturbance grows into congested flow as the stability condition is not satisfied. In the stable region, kink density waves disappear, and traffic flow becomes uniform for larger value of reaction coefficient in the corresponding pattern 2e. The region of free flow turns wide, and the amplitude of density waves is weakened with the increase in reaction coefficient which means that optimal current difference effect enhances the stability of the traffic flow.

Figure 3 represents the phase space plot of density difference  $\rho(t) - \rho(t - 1)$  against  $\rho(t)$  for  $t = 60000s - 70000s$ , corresponding to the panel of Fig. 2.

The patterns in Fig. 3a–d exhibit the characteristic of periodicity in the form of limit cycle, and the nodes on the right as well as on left sides are corresponding to the traffic states within and out of the kink traffic jam. For  $\lambda = 0.4$ , the limit cycle leads to a single point which represents the uniform flow in the stable region. When  $a = 1.5$ , the jamming transition occurs among freely moving phase, the coexisting phase with kink–antikink density wave, and the uniformly congested phase with an increase in the value of  $\lambda$ . These findings are in agreement with the results found in Refs. [19,20].

Now, we study the traffic behavior for equal configuration of vehicles for smaller value of the sensitivity. Figure 4 shows the traffic pattern at time  $t = 60000s$  for different values of  $\lambda$  at  $a = 0.75$ . It is clear from the Fig. 4a–c that the traffic pattern for smaller value of  $a$  is quite different for those obtained for larger value of  $a$ . Here, initial disturbance evolves into irregular density waves and in time, these density waves propagate backward, break up, coalesce with one another, disappear, and created till  $\lambda = 0.2$ . On further increasing the value of  $\lambda$ , these irregular density waves lead to kink–antikink density waves as shown in Fig. 4d–e. The amplitude of irregular density waves decreases with an increase in  $\lambda$ , and for  $\lambda \geq 0.3$ , the chaotic density wave evolves into kink density wave with further decrease in amplitude.

Figure 5 represents the phase space plot of density difference  $\rho(t) - \rho(t - 1)$  against  $\rho(t)$  for  $t = 60000s - 70000s$ , corresponding to the traffic flows in Fig. 4. The traffic pattern exhibits the chaotic behavior as shown in Fig. 5a–c for smaller value of  $\lambda$ . This chaotic flow is represented by the set of dispersed points in phase–space plot which is the characteristic of chaos. The chaotic pattern becomes periodic in form of limit cycle for larger value of  $\lambda$  as shown in Fig. 5d, e. Here, jamming transitions occur among freely moving phase, kink phase with kink–antikink density wave, chaotic phase with irregular density wave, and uniformly congested phase. It is worth to mention that the chaotic phase was neither observed in the triangular [20] nor in square [19] lattices for equal configuration of vehicles.

Now, we examine the boundaries of different phases in space  $(a_c, \lambda)$ . Figure 6a represents the plot of critical sensitivity against reaction coefficient, where solid (dotted) curves correspond to theoretical (numerical) results for equal configuration of vehicles. It is clear from the figure that free flow region enlarges with an increase in  $\lambda$ . The chaotic region reduces till  $\lambda = 0.3$ ,

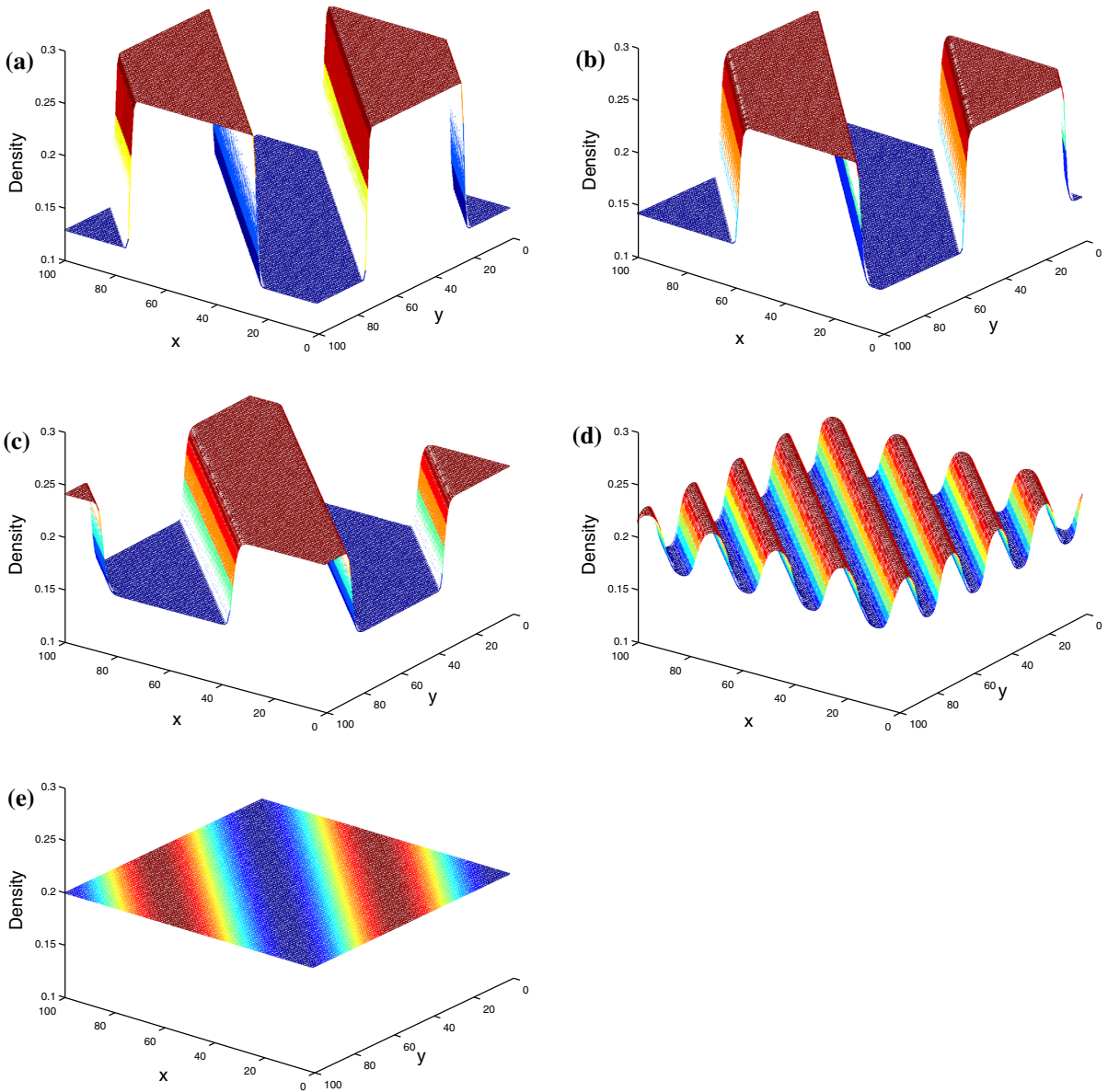


**Fig. 2** Traffic pattern at  $t = 60000$  when  $c_x = c_y = c_r = \frac{1}{3}$  and  $a = 1.5$  for **a**  $\lambda = 0$ , **b**  $\lambda = 0.1$ , **c**  $\lambda = 0.2$ , **d**  $\lambda = 0.3$ , and **e**  $\lambda = 0.4$ , respectively

and for further increase in reaction coefficient, the chaotic region remains constant. Therefore, reaction coefficient plays an important role in stabilizing the traffic flow for all values of sensitivity.

**Case 2**  $c_y = c_r \neq c_x$

Here, the fractions of vehicles in  $y$  and along diagonal direction are same, but differ from that in  $x$ -direction. In this configuration, we find only one type of jamming transition for all values of sensitivity. Here,

the jamming transitions occur from the uniform traffic flow, through the chaotic flow to the uniformly congested phase for all values of  $\lambda$ . Below the critical sensitivity, the initial small perturbation evolves into irregular density waves, and the chaotic region shrinks with an increase in the value of  $\lambda$ . When we enter into the stable region, the irregular density waves disappear and traffic flow becomes uniform for any value of reaction coefficient. Moreover, there does not exist

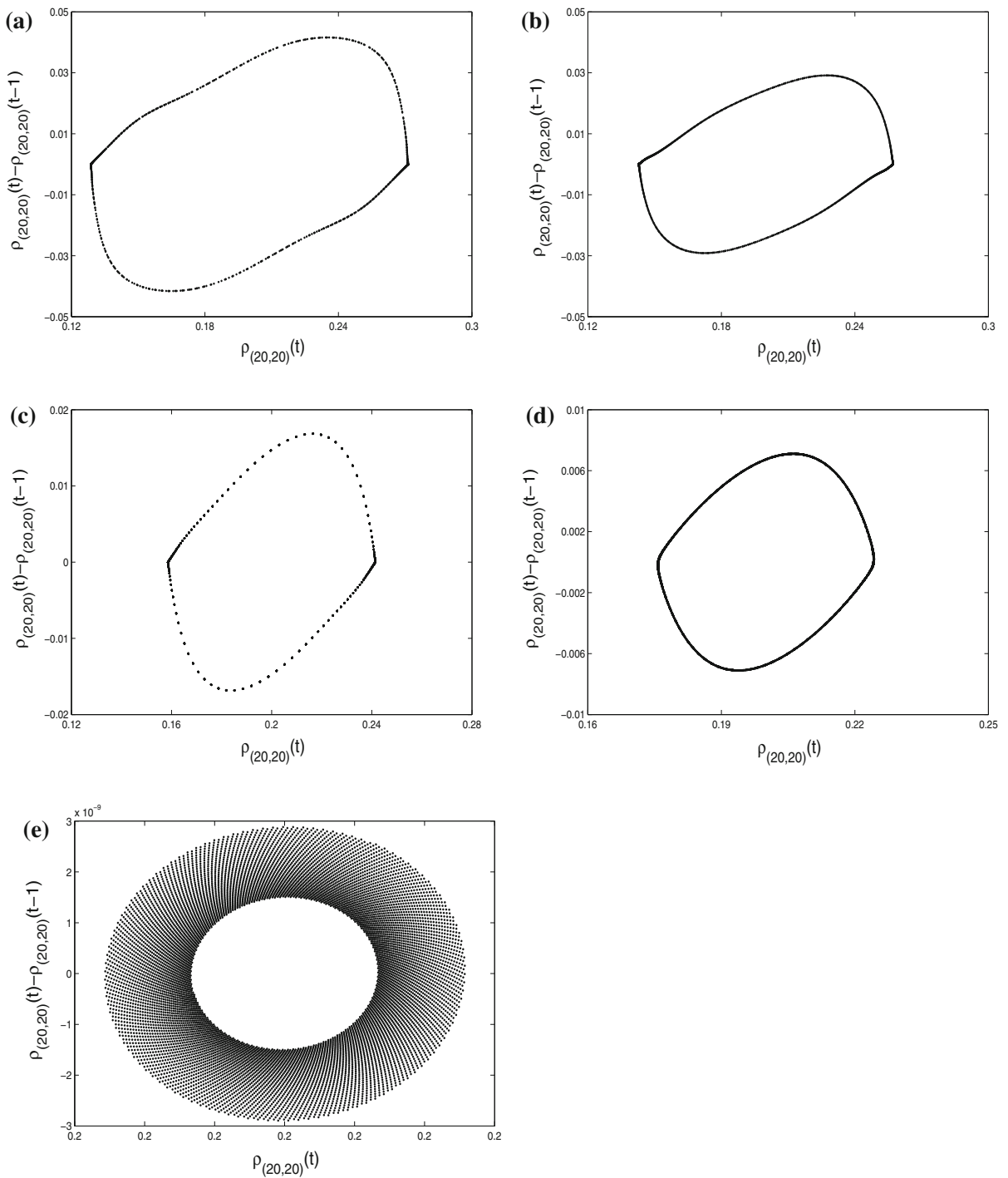


**Fig. 3** Phase space plot between time  $t = 60000 - 70000$  when  $c_x = c_y = c_r = \frac{1}{3}$  and  $a = 1.5$  for **a**  $\lambda = 0$ , **b**  $\lambda = 0.1$ , **c**  $\lambda = 0.2$ , **d**  $\lambda = 0.3$ , and **e**  $\lambda = 0.4$ , respectively

kink–antikink density wave in the unstable region. The results obtained are in accordance with those found in Ref. [20].

**Case 3**  $c_x = c_y \neq c_r$

Parallel to the case 1, here, we also observed two distinct types of jamming transitions. For larger value



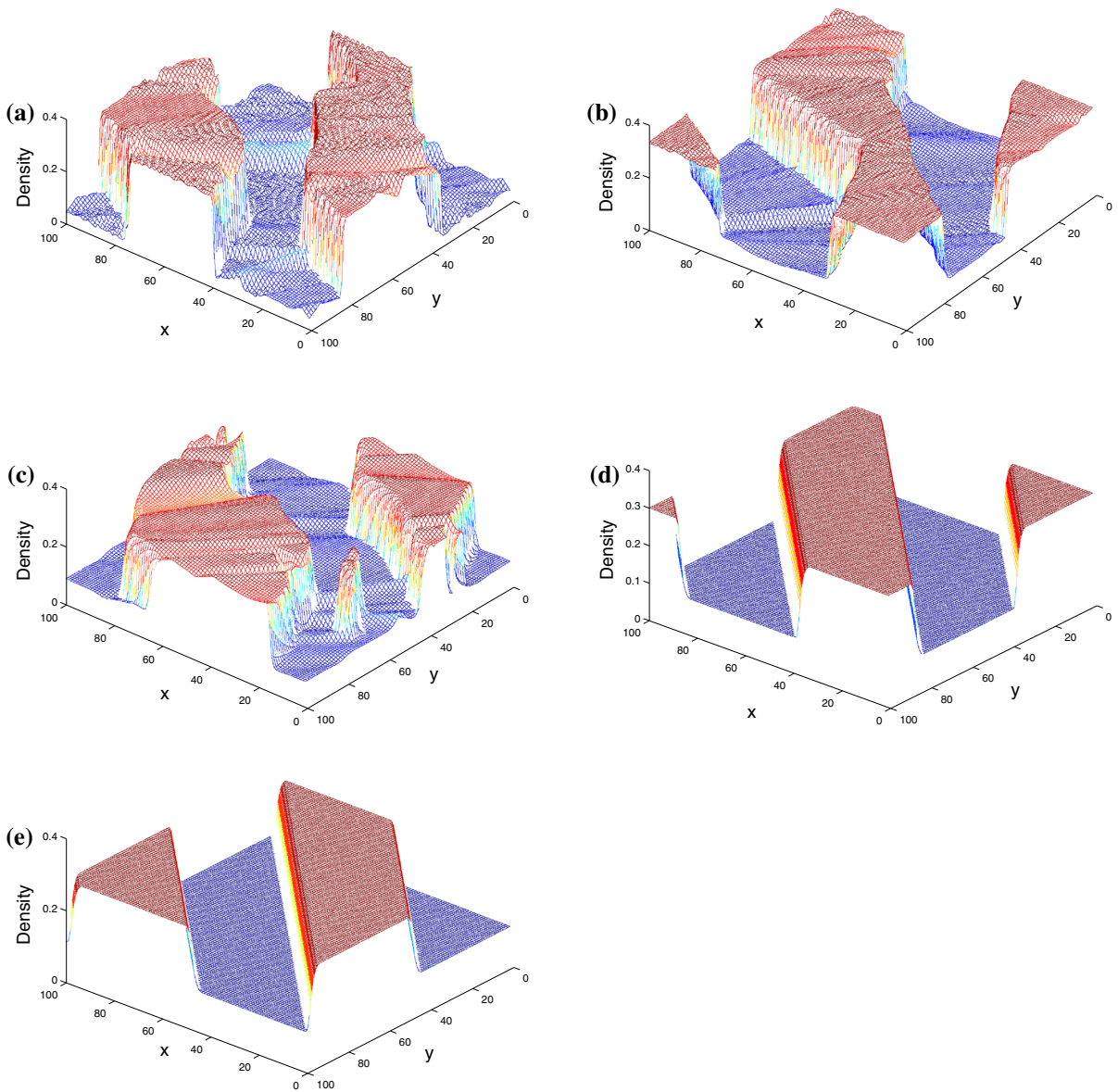


**Fig. 4** Traffic pattern at  $t = 60000$   $t = 60000 - 70000$  when  $c_x = c_y = c_r = 1/3$  and  $a = 0.75$  for **a**  $\lambda = 0$ , **b**  $\lambda = 0.1$ , **c**  $\lambda = 0.2$ , **d**  $\lambda = 0.3$ , and **e**  $\lambda = 0.4$ , respectively

of sensitivity, the jamming transition occurs from uniform traffic flow to kink density wave flow. The jamming transition arises from freely moving flow, through kink density wave flow, to chaotic density waves, for smaller value of sensitivity.

Now, we examined our results for two subcases: (a)  $c_x < c_r$  and (b)  $c_x > c_r$ . The free flow region enlarges with an increase in  $\lambda$  in both the subcases as shown in Fig. 6b, where solid and dotted curve correspond to the-

oretical and numerical results for subcase (a) and (b). The theoretical curve for subcase (a) is slightly different from subcase (b) while there is a significant difference between the chaotic boundaries. It is clear from the figure that chaotic region reduces up to a critical value of reaction coefficient. Further, an increase in the reaction coefficient does not affect the chaotic region. This critical value depends upon the fraction of vehicles moving along diagonal direction. On comparing the results of

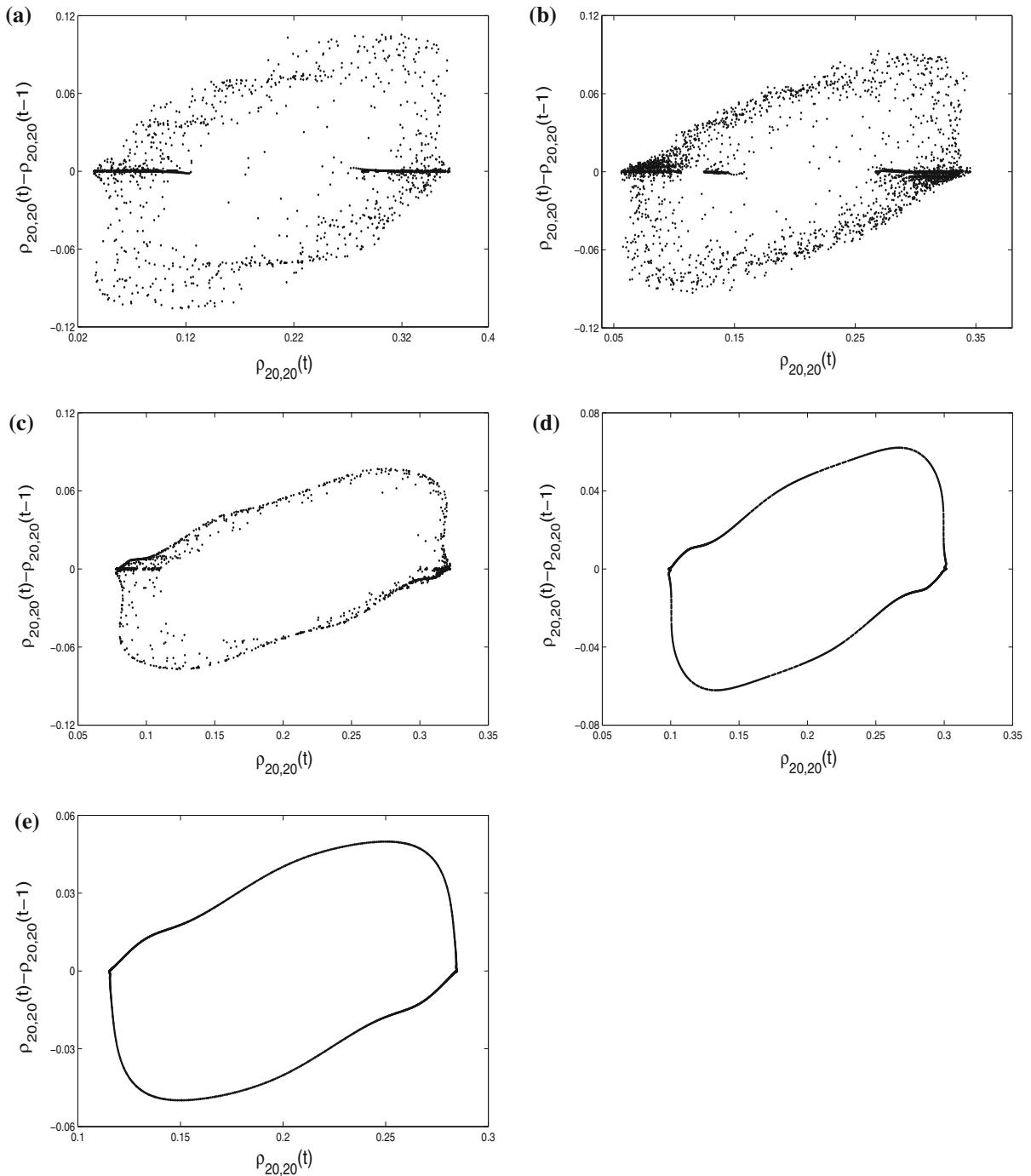


**Fig. 5** Phase space plot between time  $t = 60000 - 70000$  when  $c_x = c_y = c_r = 1/3$  and  $a = 0.75$  for **a**  $\lambda = 0$ , **b**  $\lambda = 0.1$ , **c**  $\lambda = 0.2$ , **d**  $\lambda = 0.3$ , and **e**  $\lambda = 0.4$ , respectively

two subcases, it is found that chaotic region in subcase (a) is more than subcase (b), i.e., more number of vehicles move along diagonal more will be the chaotic

region. The above type of jamming transition was not observed by Nagatani [20]. It is reasonable to conclude that chaotic region significantly depends on the num-

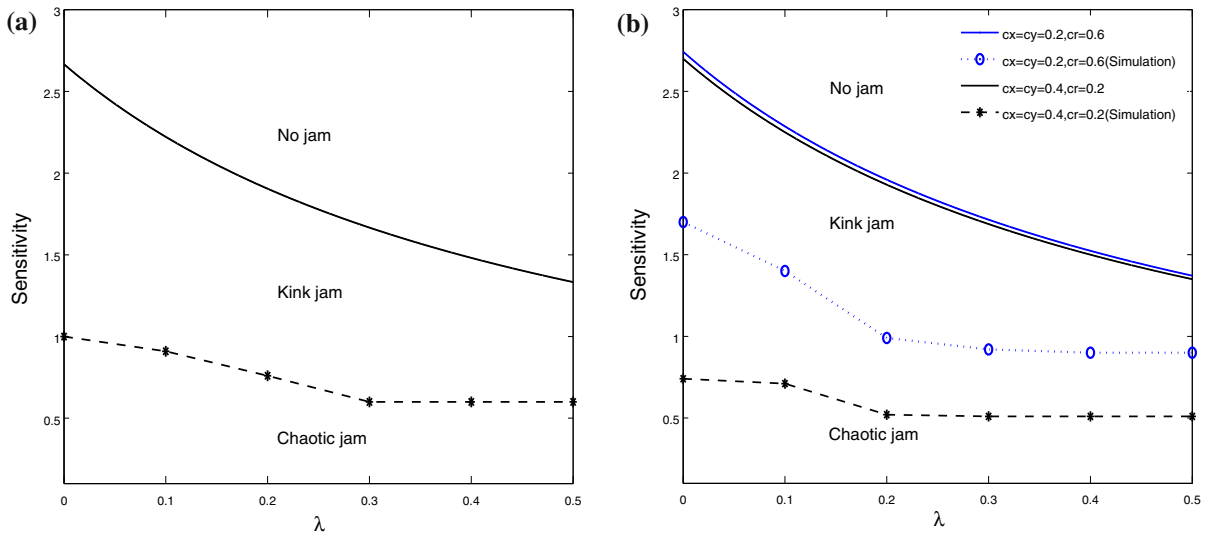


**Fig. 6** Plot of  $a_c$  against reaction coefficient  $\lambda$  for **a**  $c_x = c_y = c_r$  and **b**  $c_x = c_y \neq c_r$ , respectively

ber of vehicles moving along diagonal as well as on reaction coefficient.

**6 Conclusion**

In this letter, the effect of optimal current difference is investigated theoretically as well as numerically on a two-dimensional triangular lattice hydrodynamic traffic flow model. Different types of phase transitions are discussed, and phase diagram is presented for three different configurations of vehicles. We summarize our finding as follows:

1. The optimal current difference effect effectively stabilizes the traffic flow for any possible configuration on a triangular lattice.
2. When  $c_x = c_y = c_r$ , depending on the sensitivity for any value of reaction coefficient, two distinct types of jamming transitions occur: (a) For larger value of sensitivity, conventional jamming transition occurs from uniform traffic flow to kink density waves; (b) For smaller value of sensitivity, the jamming transitions occur from the uniform flow, through the kink jam and to the chaotic jam.
3. When  $c_y = c_r \neq c_x$ , for any value of reaction coefficient, only one type of jamming transition from uniform flow to chaotic jam occurs below the critical sensitivity.
4. When  $c_x = c_y \neq c_r$ , two distinct jamming transitions occur depending on the sensitivity similar

to as found in the case of  $c_x = c_y = c_r$ . It is also observed that chaotic flow region also depends on the fraction of vehicles moving along diagonal direction.

Finally, we concluded that the jamming transition depends on the configuration of vehicles, lattice type, and sensitivity. Simulation results obtained are also in good agreement with the theoretical findings which verify that our consideration is reasonable.

**Acknowledgments** The first author acknowledges the Council of Scientific and Industrial Research (CSIR), India for providing financial assistance.

**References**

1. Bando, M., Hasebe, K., Nakyama, A., Shibata, A., Sugiyama, Y.: Dynamical model of traffic congestion and numerical simulation. *Phys. Rev. E* **51**, 1935 (1995)
2. Jiang, R., Wu, Q.S., Zhu, Z.J.: A new continuum model for traffic flow and numerical tests. *Transp. Res. Part B* **36**, 405 (2002)
3. Gupta, A.K., Katiyar, V.K.: Analyses of shock waves and jams in traffic flow. *Phys. A* **38**, 4069 (2005)
4. Tang, T.Q., Huang, H.J., Shang, H.Y.: A new macro model for traffic flow with the consideration of the drivers forecast effect. *Phys. Lett. A* **374**, 1668 (2010)
5. Nagatani, T.: TDGL and MKdV equations for jamming transition in the lattice models of traffic. *Phys. A* **264**, 581 (1999)
6. Gupta, A.K.: Gupta, Redhu, P.: Analyses of the drivers anticipation effect in a new lattice hydrodynamic traffic flow model with passing. *Nonlinear Dyn.* (2013). doi:[10.1007/s11071-013-1183-2](https://doi.org/10.1007/s11071-013-1183-2)

7. Gupta, A.K., Redhu, P.: Analyses of drivers anticipation effect in sensing relative flux in a new lattice model for two-lane traffic system. *Phys. A* **392**, 5622 (2013)
8. Tang, T.Q., Li, C.Y., Huang, H.J.: A new car-following model with the consideration of the drivers forecast effects. *Phys. Lett. A* **374**, 3951 (2010)
9. Gupta, A.K., Redhu, P.: Analysis of a modified two-lane lattice model by considering the density difference effect. *Commun. Nonlinear Sci. Numer. Simul.* **19**, 1600 (2013)
10. Nagatani, T.: Modified KdV equation for jamming transition in the continuum models of traffic. *Phys. A* **261**, 599 (1998)
11. Ge, H.X., Cheng, R.J.: The backward looking effect in the lattice hydrodynamic model. *Phys. A* **387**, 6952 (2008)
12. Peng, G.H., Cai, X.H., Cao, B.F., Liu, C.Q.: Non-lane-based lattice hydrodynamic model of traffic flow considering the lateral effects of the lane width. *Phys. Lett. A* **375**, 2823 (2011)
13. Tian, J.F., Yuan, Z.Z., Jia, B., Li, M.H., Jiang, G.J.: The stabilization effect of the density difference in the modified lattice hydrodynamic model of traffic flow. *Phys. A* **391**, 4476 (2012)
14. Peng, G.H., Cai, X.H., Liu, C.Q., Tuo, M.X.: A new lattice model of traffic flow with the anticipation effect of potential lane changing. *Phys. Lett. A* **376**, 447 (2012)
15. Peng, G.H.: A new lattice model of two-lane traffic flow with the consideration of optimal current difference. *Commun. Nonlinear Sci. Numer. Simul.* **265**, 297 (2012)
16. Biham, O., Middelton, A.A., Levine, D.A.: Self-organization and a dynamical transition in traffic-flow models. *Phys. Rev. A* **46**, R6124 (1992)
17. Nagatani, T.: Jamming transition in a two-dimensional traffic flow model. *Phys. Rev. E* **59**, 4857 (1999)
18. Nagatani, T.: Jamming transition of high-dimensional traffic dynamics. *Phys. A* **272**, 592 (1999)
19. Gupta, A.K., Redhu, P.: Jamming transition of a two-dimensional traffic dynamics with consideration of optimal current difference. *Phys. Lett. A* **377**, 2027 (2013)
20. Nagatani, T.: Jamming transition in traffic flow on triangular lattice. *Phys. A* **271**, 200 (1999)